Green Chemistry

ROYAL SOCIETY OF CHEMISTRY

COMMUNICATION

View Article Online
View Journal | View Issue

Check for updates

Cite this: *Green Chem.*, 2024, **26**, 11860

Received 7th September 2024,
Accepted 4th November 2024

DOI: 10.1039/d4gc04481a

rsc.li/greenchem

Efficient decomposition of a melamine–formaldehyde foam into melamine *via* selective disconnection of bonds†

Chaohui Yang,[a,b,c] Xinyu Li,[a,b,c] Hongyan Li,[a,b,c] Chizhou Wang,[a,b,c] Qianqian Xing,[a,b,c] Xiaoliang Jia,[a,b,c] Xiaojing Cui,*[d] Xianglin Hou*[a,b,c] and Tiansheng Deng *[a,b,c]

The precise disconnection of one type of chemical bond in polymers realizes high-yield recovery of valuable chemicals. In this study, we demonstrate a sustainable and efficient strategy to selectively cleave the specific $sp^3C–sp^3N$ bond of a thermoset melamine–formaldehyde foam, by which valuable melamine of 99.5% purity was obtained with a yield of 95.3%.

The recovery of high value-added chemicals from waste plastics is of great significance for the plastic recycling industry and environmental management.[1] Melamine formaldehyde (MF) resin is a thermoset resin made by the polymerization of melamine and formaldehyde, in which melamine are interlinked *via* dimethyl ether bonds (pH > 9), forming a reticular network (Fig. 1).[2] MF resin has been widely applied in vehicle manufacturing, home decoration, daily cleaning products and other fields.[3] The widespread production and utilization of MF resin inevitably causes the fast accumulation of the end-of-life MF resin waste, causing environmental protection problems.[4] Developing an effective MF resin recovery method is crucial to address the issue. However, thermosetting MF resin has good thermal and chemical stability, making its degradation a challenge.[5]

Presently, the primary methods for recovering thermosetting resins include mechanical, thermal, and chemical processes.[6] The process of mechanical recycling involves pulverizing scrap resin into powders of specified particle size and utilizing it directly as one of the feedstocks for composite materials or as a reinforcing agent for other resins.[7] These simplistic treatments (crushing, cutting and grinding, *etc.*) of MF resin in the mechanical method difficult the fully utilization of the high-value units within the structure of MF resin. In the thermal recovery method, waste resins are commonly decomposed into low-molecular-weight oil or gas products at elevated temperatures.[8] This process facilitates the irregular breaking of the chemical bonds within the resin, complexing product distributions and the subsequent product separation process. Additionally, the release of toxic gases is unavoidable in the thermal recycling process.[9] Alternatively, the chemical recovery process involves the cleavage of the chemical bonds of the resin in a degradation system under relatively mild reaction conditions.[10] It is ideal but challenging to develop an efficient and green degradation system, in which the specific chemical bonds in the resins can be selectively cleaved, yielding monomers that can be easily separated and recycled. Noticeably, the majority of chemical bonds existing in MF resin are the C–N bonds of different types, including the $sp^2C–sp^2N$ bond in the 1,3,5-triazine (Tr) ring, the $sp^2C–sp^3N$ bond on the Tr ring, and the neighbouring $sp^3C–sp^3N$ bond (see Fig. 1). These C–N bonds have similar chemical activities. Hence, it remains a great challenge to selectively break one type of C–N bond without destroying the other types of C–N bonds.

[a]*State Key Laboratory of Coal Conversion, Institute of Coal Chemistry, Chinese Academy of Sciences, 27 South Taoyuan Road, Taiyuan, 030001, People's Republic of China. E-mail: dts117@sxicc.ac.cn, houxianglin@sxicc.ac.cn*
[b]*Center of Materials Science and Optoelectronics Engineering, University of Chinese Academy of Sciences, Beijing, 100049, People's Republic of China*
[c]*CAS Key Laboratory of Carbon Materials, Institute of Coal Chemistry, Chinese Academy of Sciences, 27 South Taoyuan Road, Taiyuan, 030001, People's Republic of China*
[d]*Institute of Interface Chemistry and Engineering, Department of Chemistry and Chemical Engineering, Taiyuan Institute of Technology, Taiyuan, Shanxi, 030008, People's Republic of China. E-mail: cxjtyut@126.com*

†Electronic supplementary information (ESI) available. See DOI: https://doi.org/10.1039/d4gc04481a

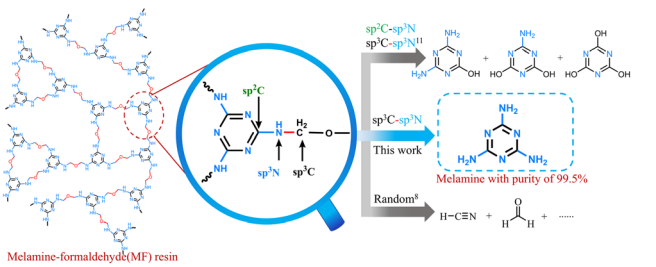

Fig. 1 Structure of MF resin and products formed by the cleavage of different types of chemical bonds.

H^+ or OH^- ions in acid or base catalysts can disconnect the C–N bonds in polymers. This bond disconnection is commonly non-selective due to the high catalytic activity of H^+ or OH^- ions. Wu *et al.*[11] applied the acid or base recovery system, *i.e.*, the methane sulfonic acid-tetrahydrofuran-10wt% H_2O or 10wt% NaOH–H_2O, to cleave the C–N bonds of MF resin. They found that either the acid or base system disconnected the sp^2C–sp^3N and sp^3C–sp^3N bonds of MF resin, producing a blend of ammelide and ammeline. If a catalytic system enables the precise cleavage of the sp^3C–sp^3N bond without influencing the other types of C–N bonds, the main products will be melamine instead of a complex mixture of ammelide and ammeline. In such a case, the product separation will be largely simplified. Surprisingly, we report herein NH_3·H_2O as a selective and efficient system to precisely cleave the sp^3C–sp^3N bond of melamine formaldehyde resin foam (MFF) with 100% selectivity to recover melamine of high purity (99.5%) with a high yield of 95.3% (entry 9, Table 1). Besides sound-absorbing MFF, other two types of commercial MFFs, namely the flame-retardant melamine compression foam and the cleaning-type melamine foam, can be efficiently degraded to melamine in the NH_3–H_2O system, showing high melamine yields of 94.8% and 93.1%, respectively (entries 27, 28, Table 1 and Fig. S1, ESI†). Compared with the previous MF resin degradation technology,[11] in this work, NH_3 was used as a catalyst, and it is a more ecologically environment-friendly substance (raw material for chemical fertilizer production). A high-purity melamine monomer was obtained instead of a hard-to-separate mixture of ammelide and ammeline. NH_3 can be separated directly through volatilization, product melamine is insoluble in H_2O and can be directly obtained, the post-treatment process is simple, compared with the post-treatment of products in previous work, and this work greatly reduces the consumption of energy and resources. Therefore, the NH_3·H_2O system degradation of MF resin is greener and more efficient (Table S1, ESI†).

When degraded in the 27 wt% ammonia solution (NH_3·H_2O), the white foam-like MFF gradually disappeared and a yellow crystal product precipitated from the aqueous system after the degradation reaction (Fig. 2a). The crystal product was characterized by NMR and IR analysis. The ^{1}H- and ^{13}C-NMR spectra of product showed a single unipolar peak at chemical shifts of 6.13 ppm and 167.5 ppm, respectively, which was identical to that of the melamine standard (Fig. 2b and c). Besides, the IR spectrum of solid product was similar to that of the melamine standard, showing the peaks for the N–H bond on the NH_2 group exterior to Tr (at 3467 cm^{-1} and 3413 cm^{-1}) and for the triazine (Tr) ring (at 1528 cm^{-1}, 1423 cm^{-1} and 809 cm^{-1}). The IR analysis is in good agreement with the NMR result, identifying the solid

Table 1 Decomposition of MFF[a]

Entry	System	System mass/g	Temp/°C	Time/h	R_d [b]/%	Y_{ma} [c]/%
1	27wt% NH_3–H_2O	3.00	170	12	100	93.8
2	27wt% $(NH_4)_2CO_3$–H_2O	3.00	170	12	100	90.3
3	27wt% Urea–H_2O	3.00	170	12	100	89.6
4	27wt% $(NH_4)_2SO_4$–H_2O	3.00	170	12	100	67.1
5	27wt% NH_4Cl–H_2O	3.00	170	12	100	27.8
6	27wt% NH_3–H_2O	2.00	170	12	100	94.5
7	27wt% NH_3–H_2O	1.00	170	12	100	95.1
8	27wt% NH_3–H_2O	0.50	170	12	100	94.6
9	27wt% NH_3–H_2O	0.15	170	12	100	95.3
10	27wt% NH_3–H_2O	0.05	170	12	100	89.4
11	27wt% NH_3–H_2O	0.15	170	4	100	65.4
12	27wt% NH_3–H_2O	0.15	170	6	100	87.4
13	27wt% NH_3–H_2O	0.15	170	8	100	89.9
14	27wt% NH_3–H_2O	0.15	170	10	100	91.6
15	27wt% NH_3–H_2O	0.15	160	12	100	84.9
16	27wt% NH_3–H_2O	0.15	150	12	100	81.9
17	27wt% NH_3–H_2O	0.15	140	12	92.6	63.7
18	NaOH–H_2O (pH = 13.5)	3.00	170	12	2.7	0
19	KOH–H_2O (pH = 13.5)	3.00	170	12	3.5	0
20	5wt% NaOH–H_2O	3.00	170	12	92.1	0
21	30wt% Na_2CO_3–H_2O	3.00	170	12	1.2	0
22	30wt% K_2CO_3–H_2O	3.00	170	12	1.9	0
23 [d]	NH_3 (1 MPa)	—	170	12	3.2	0
24	H_2O	3.00	170	12	1.9	0
25 [e]	27wt% NH_3–H_2O	3.00	170	12	0	>99
26 [f]	27wt% EDA–H_2O	3.00	170	12	100	92.1
27 [g]	27wt% NH_3–H_2O	0.15	170	12	100	94.8
28 [h]	27wt% NH_3–H_2O	0.15	170	12	100	93.1

[a] Reaction conditions: 10 ml Teflon-lined reactor, MFF: 0.15 g. [b] Degradation ratio = $(m_0 - m_1)/m_0$, where m_0 and m_1 are the mass of original MFF and residue MFF after degradation, respectively. [c] Melamine yield = $(m_2 - m_3)/(m_0 \times 0.65)$, where m_2 is the mass of the product after drying to remove NH_3·H_2O after the reaction and m_3 is the quality of the remaining insoluble solid after the dried product was dissolved in DMSO, and 0.65 in the equation represents the theoretical mass of melamine rings in 1 g of MFF. [d] Reaction pressure: 1.2–1.4 MPa, greater than the reaction pressure (0.4 MPa) in entry 9. [e] Reactant was melamine standard (0.15 g), no MFF. [f] EDA is ethylenediamine. [g] Reaction condition: 0.15 g flame-retardant-type MFF. [h] Reaction condition: 0.15 g cleaning-type MFF.

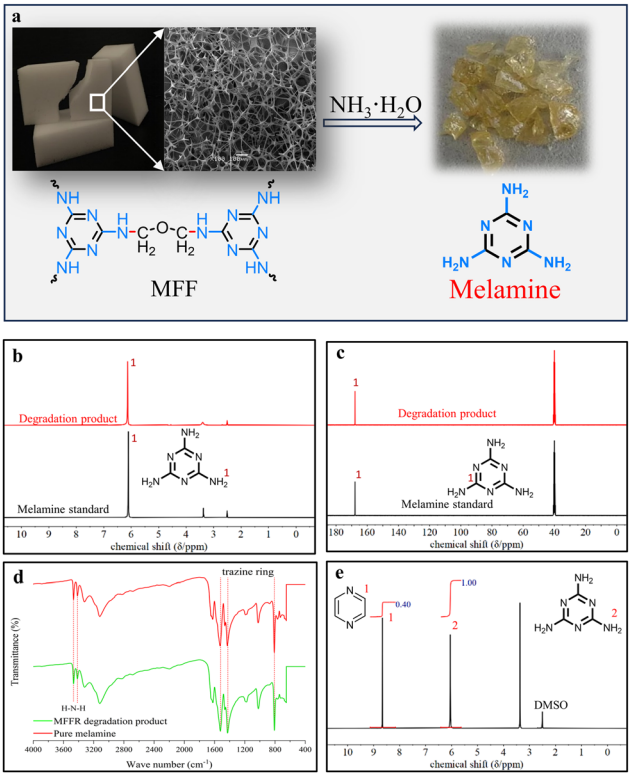

Fig. 2 (a) MFF depolymerization in $NH_3{\cdot}H_2O$ to produce a yellow transparent melamine crystal. (b) ^{1}H NMR spectrum of the MFF degradation product in $NH_3{\cdot}H_2O$ and melamine standard. (c) ^{13}C NMR spectrum of the MFF degradation product in $NH_3{\cdot}H_2O$ and melamine standard. (d) FT-IR spectrum of the MFF degradation product in $NH_3{\cdot}H_2O$ and melamine standard. (e) Nuclear magnetic quantification of MFF degradation products in $NH_3{\cdot}H_2O$, the mass of the melamine product is 10.6 mg and the quality of piperazine is 4.1 mg. Deuterated reagent of all NMR analytic is DMSO-d_6.

crystal product as melamine (Fig. 2d). In addition, the side products in the degradation solution were analyzed by ^{1}H- and ^{13}C-NMR characterizations. As displayed in Fig. S3 and S4,† the side products were either volatile or unstable molecules such as methanol, methylamine, dimethyl ether, and diamine methyl ether, their content was very low in the degradation solution.

On the basis of ^{1}H-NMR analysis, a high selectivity to melamine (99.5%) and a yield (93.8%) were obtained in 27 wt% $NH_3{\cdot}H_2O$ (entry 1, Table 1). Besides the product yield, the product purity is a key factor affecting the efficiency of whole degradation process. The purity of melamine product was determined by ^{1}H-NMR quantitative analysis (Fig. 2e).[12] The result showed that the melamine product had a purity as high as 99.5%. The elemental analysis showed that the content of C, N and H elements in the melamine product (28.57%C, 65.94%N and 4.83%H) was very close to those in the melamine standard (28.58%C, 66.55%N and 4.80%H) (Table S2, ESI†), further proving the melamine product of high purity. The high yield and purity of melamine will benefit the application of $NH_3{\cdot}H_2O$ in the industrial degradation of MFF.

Several types of aqueous ammonium salt solutions with the same mass concentration to $NH_3{\cdot}H_2O$, were also employed for the degradation reaction (entries 2–5, Table 1). They all exhibited activity for the degradation reaction, resulting in the melamine yield ranging from 27.8% to 90.3%. These ammonium salts decomposed at the reaction temperature to produce NH_3, as indicated by the pungent NH_3 smell after reaction. These released NH_3 enabled the decomposition of MFF. Noticeably, $NH_3{\cdot}H_2O$ showed a higher melamine yield than the ammonium salt solutions. $NH_3{\cdot}H_2O$ can release NH_3 directly without the salt decomposition step, accelerating the reaction. Moreover, it did not have the anions existed in the ammonium salts, including CO_3^{2-}, SO_4^{2-}, and Cl^-. In such case, the possible negative effect of these anions on the degradation reaction can be avoided.

Furthermore, the impact of reaction conditions on the degradation reaction was explored, including the $NH_3{\cdot}H_2O$ amount, the reaction time and reaction temperature. A reduction of $NH_3{\cdot}H_2O$ amount from 3.00 g to 0.15 g led to the same melamine selectivity and comparable melamine yield, whereas a further decrease in $NH_3{\cdot}H_2O$ amount to 0.05 g resulted in a declined degradation efficacy (entries 1, 6–10, Table 1). The highest melamine yield of 95.3% was reached with the $NH_3{\cdot}H_2O$ amount of 0.15 g. Hence, the effects of reaction time and temperature on the degradation reaction were studied with 0.15 g of $NH_3{\cdot}H_2O$ (entries 9, 11–14 and 15–17, Table 1). An increased reaction time and an elevated reaction temperature enhanced the MFF degradation reaction.

$NH_3{\cdot}H_2O$ (27wt%) was alkaline with a pH value of 13.5. To exclude the catalytic effect of alkaline OH^- ions on the depolymerization of MFF, the solutions of NaOH–H_2O and KOH–H_2O that have the same pH values (13.5) as that of $NH_3{\cdot}H_2O$ (27wt%), were chosen for MFF degradation. MFF did not degrade in the above two solutions (entries 18 and 19, Table 1). In addition, 5wt% NaOH–H_2O was applied to degrade MF resin under the same reaction conditions as that of $NH_3{\cdot}H_2O$ (entry 20, Table 1). The degradation rate reached 92.1%, and the products included ammelide and ammeline. Therefore, NH_3 has a higher degradation activity and a narrower product distribution than NaOH. The Na_2CO_3–H_2O (30 wt%) and K_2CO_3–H_2O (30 wt%) solutions that have similar mass concentrations to that of $NH_3{\cdot}H_2O$ were also applied to recycle MFF under the identical condition, both of which were inert toward MFF degradation (entries 21 and 22, Table 1). NH_3 or H_2O alone was employed to react with MFF, and neither of them can degrade MFF. This result suggested that the degradation of MFF by $NH_3{\cdot}H_2O$ was achieved through the synergy of NH_3 and H_2O (entries 23 and 24, Table 1).

In order to further evaluate the greenness of the $NH_3{\cdot}H_2O$ system, we analyzed and compared the green metrics[13] of the $NH_3{\cdot}H_2O$ system recovery of MF resin with the previous recovery technology. The detailed information is shown in Tables S3 and S4.† Environmental impact factors (EF) and process mass intensity (PMI) were calculated respectively. The results show that simple EF, complete EF, EF, Waste amount and PMI values of the $NH_3{\cdot}H_2O$ system (1.06, 2.27, 1.06, 0.66, and 3.27)

are lower than those of the MSA–THF–H_2O system (2.36, 8.92, 2.93, 1.70, and 9.92) and NaOH–H_2O system (1.65, 11.23, 1.65, 1.03, 12.23). This proves the greenness and economy of $NH_3{\cdot}H_2O$ to degrade MF resin.

The possible reaction route was explored for the degradation of MF resin to melamine. Two routes were proposed. The first one involved the formation of melamine *via* a multi-step process, *i.e.*, MF resin degraded into ammelide, ammeline and/or cyanic acid, followed by their transformation to melamine, while in the second one, MF resin degraded directly into melamine without the above intermediate(s). Ammelide, ammeline and cyanic acid were chosen as the model reactant and tested in 27 wt% $NH_3{\cdot}H_2O$, respectively. No melamine was formed in all of the tests (Fig. S5, ESI†), which ruled out the first route as the reaction pathway. Additionally, the stability experiment showed that >99% of melamine was stable in $NH_3{\cdot}H_2O$ (entry 25, Table 1) with the structure unchanged (Fig. S6, ESI†). These results proved the second route as the reaction pathway, *i.e.*, MF resin degraded directly into melamine.

In the direct depolymerization route of MF resin, the nature of selective disconnection of C–N bond was elucidated *via* model reactions. Two possible paths existed for $NH_3{\cdot}H_2O$ to directly depolymerize MF resin into melamine (Fig. 3): path1 involved the selective breakage of the sp^3C–sp^3N bond (without breaking the sp^2C–sp^3N bond) to produce melamine, while in path 2, the ammonia molecule attacked the Tr ring, by which the sp^2C–sp^3N bond was cleaved to form melamine. It is noticed that in path 2, the cleavage of the sp^2C–sp^3N bond led to the leaving of a sp^3N atom of MF resin, and this vacancy was replenished by a N atom of NH_3. When NH_3 is replaced by ethylenediamine (EDA), the replenishment of a N atom of EDA will lead to the formation of N^2,N^4,N^6-tris(2-aminoethyl)-1,3,5-triazine-2,4,6-triamine, if path 2 is the reaction path. EDA was utilized as the model substitute for NH_3 in the $NH_3{\cdot}H_2O$ solution to cleave the C–N bond of MF resin (entry 26, Table 1). The product was identified to be melamine (Fig. S7, in ESI†), which excluded path 2 as the reaction path. Hence, path 1 was the reaction pathway.

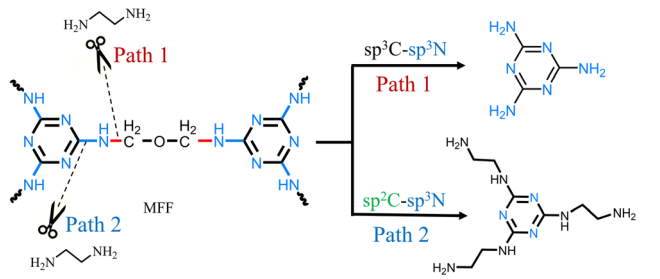

Fig. 3 Ethylenediamine replaces NH_3 in $NH_3{\cdot}H_2O$ to investigate the decomposition path of MF resin. In the degradation of MF resin to melamine, the cleavage of either NH–CH_2 (sp^3N–sp^3C) (path 1) or C–NH (sp^2C–sp^3N) bond (path 2) of MF resin is inevitable, as illustrated in Fig. 3. If the NH–CH_2 bond is cleaved, melamine will be produced (see path 1). If the C–NH bond is cleaved (see path 2), no amino group will be present outside the triazine ring. In such case, the additional amino groups will be needed to produce melamine. These additional amino groups can only come from ethylenediamine (NH_2–CH_2–CH_2–NH_2). As a result, the amino groups outside the triazine ring will be NH_2–CH_2–CH_2–NH_2 groups, producing N^2,N^4,N^6-tris(2-aminoethyl)-1,3,5-triazine-2,4,6-triamine as the product (other than melamine).

It is essential for $NH_3{\cdot}H_2O$ to interact with MF resin before it cleaves the C–N bond of MF resin. The interaction between $NH_3{\cdot}H_2O$ and MF resin was explored by ^{13}C-NMR characterization, in order to understand how $NH_3{\cdot}H_2O$ initiate the cleavage of C–N bond. For a simple and accurate analysis, MF resin prepolymer that has the typical structure unit of MF resin was chosen as to model MF resin (Fig. S8, ESI†). MF resin prepolymer itself and its mixture with $NH_3{\cdot}H_2O$ were analyzed by ^{13}C-NMR (Fig. S9, ESI†). MF resin prepolymer has two distinct types of C atoms, *i.e.*, the sp^2 C atoms (located at the Tr ring) and sp^3 C atoms (located at the chains). Both sp^2 C and sp^3 C were neighbored by N atom(s). Notably, the presence of $NH_3{\cdot}H_2O$ caused a movement of chemical shift (δ) of the two types of C atoms towards the high δ direction, indicating the decrease in the electron cloud density of the two types of C atoms. This result implied that the C atoms were surrounded by more electron-withdrawing atoms, *i.e.*, N and O atoms of $NH_3{\cdot}H_2O$. It is possible that the N and O atoms of NH_3 and H_2O can associate with the H, O and N atoms of MF resin prepolymers *via* hydrogen bonds (O–H···N, N–H···N, and N–H···O, *etc.*) to form a stable six-ring structure (Fig. S10, ESI†). In this six-ring structure, the electron transfer from the C atoms of the MF resin prepolymer to the N and O atoms of NH_3 and H_2O was achieved *via* an inductive effect.

Additionally, ^{13}C-NMR characterization was employed to probe the alterations in chemical bonds during the degradation of MF resin at a microscopic level (Fig. S11, ESI†), 0.15 g of MF resin was degraded in 3 g of $NH_3{\cdot}H_2O$ at 170 °C with different reaction periods (3 h, 6 h, and 9 h), and the resulting degradation solution was directly characterized by ^{13}C-NMR. The degradation of MF resin became increasingly intensive as the reaction time progressed. At 3 h, Tr–NH_2 groups and Tr–NH–CH_2–O–CH_2–NH–Tr groups were dominant in the degradation system, whereas Tr–NH–CH_2–OH groups were scarce and few. As the reaction time prolonged, the content of Tr–NH_2 groups increased progressively, accompanied by the significant diminishing of Tr–NH–CH_2–O–CH_2–NH–Tr groups and nearly complete consumption of Tr–NH–CH_2–OH groups. Nevertheless, NMR evidenced that the concentration of Tr–NH_2 groups was substantially higher than that of Tr–NH–CH_2–O–CH_2–NH–Tr groups at 9 h, indicating that the reaction mechanism involved the breakage of ether bonds and sp^3C–sp^3N bonds.

The degradation mechanism of MF resin was further detailed by density functional theory (DFT) on the Gaussian 16 platform (Fig. 4a).[14] The model compound, R1, which possesses a comparable structure to MF resin, was developed using Gaussview 6.0.[15] In the depolymerization process, NH_3 and R1 interacted with each other to form two hydrogen bonds, generating the intermediate species 2 with a six-membered-ring structure, and this step had an energy of

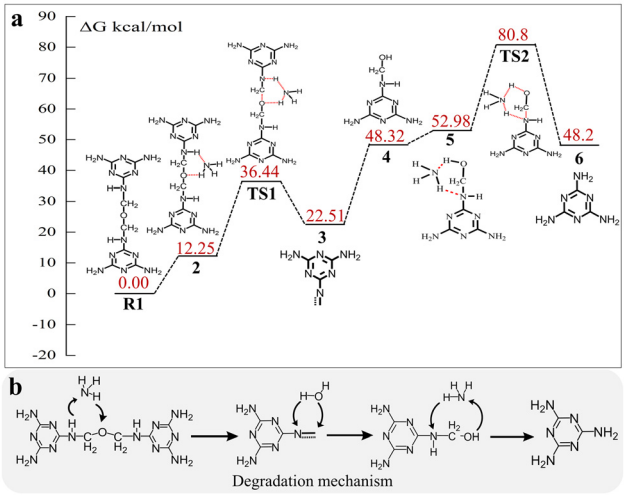

Fig. 4 (a) The changes in the structure and energy in the process of $NH_3{\cdot}H_2O$ depolymerizing MF resin were DFT calculated using the Gaussian 16 platform. (b) Degradation mechanism of MF resin.

12.25 kcal mol^{-1}. One hydrogen (H) atom of NH_3 attacked and then bound to the (O) oxygen atom of R1, meanwhile one H atom on the N atom of intermediate 2 interacted and then bounded to the N atom of NH_3, leading to the formation of intermediates 3 and 4 through the transition state TS1. The Gibbs activation energy and Gibbs reaction energy for this step were 24.19 kcal mol^{-1} and 10.26 kcal mol^{-1}, respectively. Subsequently, the additive reaction between the C═N bond of intermediate 3 and H_2O produced intermediate 4, with an activation energy of 25.81 kcal mol^{-1}. Thereafter, NH_3 and intermediate 4 interacted with each other to produce intermediate 5 *via* hydrogen bonding, showing an activation energy of 4.66 kcal mol^{-1}. Intermediate 5 subsequently cleaved its sp^3C–sp^3N bond to yield melamine *via* the transition state TS2 and H transfer. The Gibbs activation energy and Gibbs reaction energy for this step were 27.82 kcal mol^{-1} and −4.78 kcal mol^{-1}, respectively. Briefly, the principal process of MF resin depolymerization, as shown in Fig. 4b, started from the formation of a six-membered-ring intermediate through the H-bond association between MF resin and NH_3, followed by the breakage of ether bonds and sp^3C–sp^3N bonds *via* H transfer.

Conclusions

This study introduces a novel approach to utilize $NH_3{\cdot}H_2O$ to greenly and efficiently degrade MF resin. The synergy effect of NH_3 and H_2O selectively cleaved the sp^3C–sp^3N bond within MF resin without damaging the sp^2C–sp^3N bonds of MF resin at 170 °C for 12 h, by which valuable melamine was recovered with a high yield of 95.3%. The recovered melamine was precipitated from the degradation solution as crystals with a high purity of 99.5%, which simplifies largely the following product separation. Compared with previous MF resin recovery systems, in this work, the catalyst NH_3 is a more ecologically environment-friendly substance, melamine monomer insoluble in $NH_3{\cdot}H_2O$ was obtained directly, without tedious and resource-intensive post-processing, greatly reducing the consumption of resources and energy, so $NH_3{\cdot}H_2O$ system degradation MF resin is greener and more efficient. Through the comparison of EF of different systems, it is more intuitive to reflect the $NH_3{\cdot}H_2O$ system greenness and economy. A viable degradation mechanism was proposed and corroborated by combining NMR and density functional theory calculations. The ability of $NH_3{\cdot}H_2O$ to precisely cleave the specific C–N bond makes it a great candidate in the controllable recovery of high-value-added chemicals from MF resin and other polymers that contain different types of C–N bonds.

Author contributions

Chaohui Yang: data curation, investigation, and writing – original draft. Xinyu Li: methodology and software. Hongyan Li: methodology and software. Chizhou Wang: methodology. Qianqian Xing: software. Xiaoliang Jia: methodology and software. Xiaojing Cui: writing – review & editing. Xianglin Hou: resources, funding acquisition, investigation, and project administration. Tiansheng Deng: conceptualization, resources, methodology, supervision, validation, project administration, and writing – review & editing.

Data availability

The data supporting the findings of this study are available from the corresponding author upon reasonable request.

Conflicts of interest

There are no conflicts to declare.

Acknowledgements

This work was financially supported by the autonomous research project of SKLCC (Grant No.: 2024BWZ007), Fundamental Research Program of Shanxi Province (No. 202303021211257 and No. 202303021212375) and the Fund of Shanxi Province patent Transformation Special Plan Project (No. 202306005).

References

1 (*a*) J. M. Garcia and M. L. Robertson, *Science*, 2017, **358**, 870–872; (*b*) T. El Darai, A. Ter-Halle, M. Blanzat, G. Despras, V. Sartor, G. Bordeau, A. Lattes, S. Franceschi, S. Cassel, N. Chouini-Lalanne, E. Perez, C. Déjugnat and

J.-C. Garrigues, *Green Chem.*, 2024, **26**, 6857–6885; (*c*) A. Conroy, S. Halliwell and T. Reynolds, *Composites, Part A*, 2006, **37**, 1216–1222.

2 (*a*) H. Zhu and S.-A. Xu, *RSC Adv.*, 2018, **8**, 17879–17887; (*b*) Y.-Y. Pan, W.-M. Yin, R.-J. Meng, Y.-R. Guo, J.-G. Zhang and Q.-J. Pan, *RSC Adv.*, 2021, **11**, 24038–24043; (*c*) B. Song, X. Zhu, W. Wang, L. Wang, X. Pei, X. Qian, L. Liu and Z. Xu, *J. Ind. Eng. Chem.*, 2023, **119**, 130–152; (*d*) Y. Yang, Y. Deng, Z. Tong and C. Wang, *J. Mater. Chem. A*, 2014, **2**, 9994–9999.

3 (*a*) A. Khan, C. L. Y. Leon, D. A. David, A. Pacheeri, P. Sreeram, K. T. Mohammed Kenz, P. Raghavan and P. S. Owuor, *Handbook of Thermosetting Foams, Aerogels, and Hydrogels*, 2024, pp. 505–532, DOI: 10.1016/b978-0-323-99452-1.00010-3; (*b*) S. Li, W. Mo, Y. Liu and Q. Wang, *Chem. Eng. J.*, 2023, **454**, 140133; (*c*) D. J. Merline, S. Vukusic and A. A. Abdala, *Polym. J.*, 2013, **45**, 413–419.

4 (*a*) S. Chen and Y. H. Hu, *Chem. Eng. J.*, 2024, **493**, 152727; (*b*) W. S. El-Sayed, A. F. El-Baz and A. M. Othman, *Int. Biodeterior. Biodegrad.*, 2006, **57**, 75–81; (*c*) T. U. Nisa, W. A. Khokhar, U. Imran, S. A. Khokhar and N. Soomro, *Chemosphere*, 2024, **349**, 140778.

5 (*a*) T. Q. Bui, L. J. Konwar, A. Samikannu, D. Nikjoo and J.-P. Mikkola, *ACS Sustainable Chem. Eng.*, 2020, **8**, 12852–12869; (*b*) K. S. Kim, S. Y. Choi, T. W. Kim and M. J. Kang, *ACS Sustainable Chem. Eng.*, 2024, **12**, 7083–7091; (*c*) Q. Si, F. Jin and J. Yang, *New Chem. Mater.*, 2017, **45**, 125–127; (*d*) H. He, D. Meng and X. Chen, *Appl. Chem. Ind.*, 2013, **42**, 1065.

6 (*a*) F. Ruan, J. Shi, Z. Xu and J. Xing, *Text. Res. J.*, 2019, **40**, 152–157; (*b*) C. Wang, N. Zhang, S. Wu, W. Wang, P. Zhao, S. Jia, Y. Qi, X. Hou, X. Cui and T. Deng, *Compos. Sci. Technol.*, 2024, **248**, 110442; (*c*) Y. Wang, X. Cui, Q. Yang, T. Deng, Y. Wang, Y. Yang, S. Jia, Z. Qin and X. Hou, *Green Chem.*, 2015, **17**, 4527–4532; (*d*) J. J. Jiang, G. L. Deng, X. Chen, X. Y. Gao, Q. Guo, C. M. Xu and L. C. Zhou, *Compos. Sci. Technol.*, 2017, **151**, 243–251.

7 (*a*) J. M. Soto, G. Blázquez, M. Calero, L. Quesada, V. Godoy and M. A. Martín-Lara, *J. Cleaner Prod.*, 2018, **203**, 777–787; (*b*) J. Q. Pan, Z. F. Liu, G. F. Liu, S. W. Wang and H. H. Huang, *J. Cent. South Univ. Technol.*, 2005, **12**, 157–161; (*c*) P. He, Z. Wu, S. Pan, C. Chen and H. Li, *Eng. Plast. Appl.*, 2013, **41**, 42–45.

8 (*a*) W. Wang, N. Zhang, C. Wang, H. Li, S. Jia, Y. Qi, H. Fan, X. Cui, X. Hou and T. Deng, *Green Chem.*, 2023, **25**, 5213–5221; (*b*) Z. Czech and R. Pelech, *J. Therm. Anal. Calorim.*, 2010, **101**, 309–313; (*c*) L. Y. Huang, Y. Shi, X. G. Jin, Z. Q. Wu, F. M. Li and S. Z. D. Cheng, *Sci. China, Ser. B: Chem.*, 1999, **42**, 316–325.

9 (*a*) Z. Czech and R. Pelech, *Mater. Sci.*, 2009, **27**, 851–856; (*b*) S. Dattilo, C. Puglisi, E. F. Mirabella, A. Spina, A. A. Scamporrino, D. C. Zampino, I. Blanco, G. Cicala, G. Ognibene, C. Di Mauro and F. Samperi, *Polymers*, 2020, **12**, 1810; (*c*) Z. Czech and R. Pelech, *Prog. Org. Coat.*, 2010, **67**, 72.

10 (*a*) N. Hu, L. Su, H. Li, N. Zhang, Y. Qi, H. Wang, X. Cui, X. Hou and T. Deng, *Green Chem.*, 2024, **26**, 9378–9387; (*b*) P. Zhao, X. Cui, C. Wang, X. Shao, H. Li, N. Zhang, X. Hou and T. Deng, *Polym. Degrad. Stab.*, 2024, **225**, 110774; (*c*) Z. Tian, Q. Zhao, X. Liu, Y. Wang, J. Zhao, Y. Wang and X. Hou, *ACS Sustainable Chem. Eng.*, 2023, **11**, 11590–11600; (*d*) N. Zhang, S. Wu, C. Wang, X. Cui, T. Zhao, L. Yuan, Y. Qi, X. Hou, H. Jin and T. Deng, *Green Chem.*, 2022, **24**, 7395–7402.

11 (*a*) S. Wu, N. Zhang, S. Jia, C. Wang, Y. Wang, Y. Qi, H. Wang, X. Cui, X. Hou and T. Deng, *Green Chem.*, 2021, **23**, 7816–7824; (*b*) S. Wu, N. Zhang, C. Wang, X. Hou, J. Zhao, S. Jia, J. Zhao, X. Cui, H. Jin and T. Deng, *Green Energy Environ.*, 2024, **9**, 919–926.

12 H. Ma, C. M. Pedersen, Q. Zhao, Z. Lyu, H. Chang, Y. Qiao, X. Hou and Y. Wang, *Anal. Chim. Acta*, 2019, **1066**, 21–27.

13 R. A. Sheldon, *Green Chem.*, 2007, **9**, 1273–1283; R. A. Sheldon, *Green Chem.*, 2017, **19**, 18–43; F. Roschangar, R. A. Sheldon and C. H. Senanayake, *Green Chem.*, 2015, **17**, 752–768.

14 M. J. Frisch, G. W. Trucks, H. B. Schlegel, G. E. Scuseria, M. A. Robb, J. R. Cheeseman, G. Scalmani, V. Barone, G. A. Petersson, H. Nakatsuji, X. Li, M. Caricato, A. V. Marenich, J. Bloino, B. G. Janesko, R. Gomperts, B. Mennucci, H. P. Hratchian, J. V. Ortiz, A. F. Izmaylov, J. L. Sonnenberg, D. Williams-Young, F. Ding, F. Lipparini, F. Egidi, J. Goings, B. Peng, A. Petrone, T. Henderson, D. Ranasinghe, V. G. Zakrzewski, J. Gao, N. Rega, G. Zheng, W. Liang, M. Hada, M. Ehara, K. Toyota, R. Fukuda, J. Hasegawa, M. Ishida, T. Nakajima, Y. Honda, O. Kitao, H. Nakai, T. Vreven, K. Throssell, J. A. Montgomery Jr., J. E. Peralta, F. Ogliaro, M. J. Bearpark, J. J. Heyd, E. N. Brothers, K. N. Kudin, V. N. Staroverov, T. A. Keith, R. Kobayashi, J. Normand, K. Raghavachari, A. P. Rendell, J. C. Burant, S. S. Iyengar, J. Tomasi, M. Cossi, J. M. Millam, M. Klene, C. Adamo, R. Cammi, J. W. Ochterski, R. L. Martin, K. Morokuma, O. Farkas, J. B. Foresman and D. J. Fox, *Gaussian 16*, Wallingford CT, 2016, https://gaussian.com/gaussian16/.

15 R. Dennington, T. A. Keith and J. M. Millam, GaussView, Version 6, Semichem Inc., Shawnee Mission, KS, 2016, https://gaussian.com/gaussview6/.